Article

Determining the Influence of a Magnetic Field on the Vibration and Fuel Consumption of a Heavy Diesel Engine

Yousef Darvishi [1], Seyed Reza Hassan-Beygi [2,*], Jafar Massah [2], Marek Gancarz [3,4,*], Arkadiusz Bieszczad [3] and Hamed Karami [5]

1   Department of Biosystems Engineering, University of Tehran, Tehran 3391653755, Iran
2   Department Agro-Technology, College of Abouraihan, University of Tehran, Tehran 3391653755, Iran
3   Faculty of Production and Power Engineering, University of Agriculture in Kraków, Balicka 116 B, 30-149 Kraków, Poland
4   Institute of Agrophysics Polish Academy of Sciences, Doświadczalna 4, 20-290 Lublin, Poland
5   Department of Petroleum Engineering, College of Engineering, Knowledge University, Erbil 44001, Iraq
*   Correspondence: rhbeigi@ut.ac.ir (S.R.H.-B.); m.gancarz@urk.edu.pl (M.G.)

Abstract: Most of the fuels used in internal combustion engines are liquid fuels. The magnetic behavior of fuel leads to a change in the interaction of hydrocarbon and oxygen molecules. This study aimed to evaluate the fuel consumption and engine vibration (time domain) of the Perkins A63544 diesel engine using magnetized fuel. The vibration of an internal combustion engine can cause failure in engine components and discomfort and injury to users. Engine vibration behavior changes due to changes in fuel types and engine combustion. Therefore, in this study, the vibration behavior of the tractor engine (Perkins model, four-stroke, direct injection diesel) was evaluated in stationary mode at different engine speeds due to changes in fuel types. Three accelerometers (CTC AC102 model) were used to measure the vibration acceleration. The fuels used included diesel as a normal control and fuels that had been subjected to magnetic field intensities of 1000, 2000, 3000, and 4000 gauss. The longitudinal, vertical, and lateral vibration signals with 5 levels of engine speed were measured. The results illustrated that the vibration root mean square (RMS) values were essentially ($p < 0.01$) affected by the engine speed, fuel type, and their interactions. It was found that for the 4000-gauss magnetized fuel, the average vibration acceleration using the five velocity settings reduced by 15%, 15.30%, 12.40%, 12.35%, and 15.38% compared to the respective control fuels. The results showed that engine fuel consumption and specific fuel consumption decreased by 2.3% using the 4000-gauss magnetized fuel compared with the normal control fuel.

Keywords: vibration; specific fuel consumption; magnetized fuel; RMS

1. Introduction

In recent years, many approaches have been proposed to diminish fuel consumption and emissions from internal combustion engines. Emissions such as NOx and CO produced by burning fossil fuels are one of the main causes of pollution in the atmosphere. Accumulation of CO_2 and other greenhouse gases in the atmosphere is causing changes in the Earth's climate and seems to have dire consequences for humans and other organisms [1–8]. In another survey concerning the magnetic field, a two-stroke engine was utilized in the fuel line; fuel consumption diminished by about 9–14%, and CO, as well as HC pollutants, dropped by 30 and 40%, respectively [9,10]. Generally, fuels used in internal combustion engines are a combination of several molecules. These molecules are made of atoms (electrons, protons, and neutrons). Positive and negative charges in these fuels can be observed in magnetic movements. By applying a strong magnetic field, the internal levels of molecules are changed. However, because these molecules have not yet been released, they cannot react with oxygen molecules actively. Fuel molecules or chains of hydrocarbons must be ionized to be released. Ionization phenomena and the release of molecules are achieved

by applying a magnetic field [11]. Using a magnetic field, the internal energy of fuel can be increased, which means some alteration in the molecular surface of fuel leads to a rise in the internal energy of the fuel, its molecular segregation, and more reactivity, thereby improving combustion [12]. In a research study, petroleum, diesel, and gasoline fuels were situated in magnetic fields of varying intensity and duration. The results verified a 10% reduction in gasoline viscosity and a 4% fall in diesel viscosity [13]. In another study, the mechanical characteristics of the rotating system of two double disks were examined. The Hall current effect, Arrhenius activation energy, and chemical reaction entropy generation were investigated. The results showed that the time-independent three-dimensional flow of Maxwell nanofluid was induced using two parallel rotating disks because of the Hall current effect [14]. Moreover, the entropy generation in unsteady magneto-bioconvection Casson nanofluid flow in the presence of Cattaneo–Christov heat and mass flux theory was investigated. The Buongiorno nanofluid model was used to consider the influences of Brownian motion, viscous dissipation, and thermophoresis [15]. Torsional vibrations (acceleration) in engines exhibit a phenomenon that is not typical of vibrations. These effects are rooted in the geometry of the reciprocating mechanism and emerge through dynamic analysis. Apart from the fact that the system changes by crankshaft rotation, the outcomes show that torsional vibration is influenced by friction between the piston and the cylinder [16]. In another research study, the vibration of the two-wheel tractor was investigated during transportation. It was shown that when the rotational speed of the engine increases, the RMS average acceleration of vibration generally rises in all situations and gears, and the highest increase in RMS acceleration value is in light gears [17]. The present research aimed to look at the impact of magnetized fuel on the vibration function and fuel consumption of diesel engines of MF-399 tractors. In this survey, the vibration of the MF-399 tractor engine at five levels of engine rotational speed under load was measured using magnetized fuel, and the values of acceleration RMS and vibration signals were recorded.

2. Materials and Methods

2.1. Diesel Engine

In this survey, an MF399 tractor engine made by Tractorsazi Co., Tabriz, Iran, was utilized. Table 1 shows the technical characteristics of the engine during all experiments. Because the tractor was used in a stationary state, the tractor engine was the main source of vibrations. The moving parts of an engine are the crankshaft, connecting rods, and pistons. Vibration in mutual motors is caused by changes in the gas weight interior of the cylinder and substituting inertia strengths focused on diverse motor parts.

Table 1. Technical details of an MF 399 tractor engine.

Model Type	Perkins A63544
Builder	Iran tractor co.
Combustion type	Direct injection
Cylinders	6
Cylinder stroke	128 mm
Bore of cylinders	98.5 mm
Volume of cylinders	5.8 liter
Topmost power	2300 rpm, 110 hp
Topmost torque	1300 rpm, 375 N m

2.2. The Magnetizer Machine

To magnetize diesel fuel, an alternative magnetic field manufacturer with a maximum capacity of 6000 gauss was made by the agricultural and technical group of Abouraihan-Tehran University. As can be seen in Figure 1, this device contains the following main parts:

Figure 1. Magnetic fuel conditioner device. (1) Fuel tank. (2) The route of fuel rotation. (3) Power supply. (4) Cooling system.

2.3. The Vibration-Measuring Device

In this research, the vibration of the MF-399 tractor engine was estimated both in stationary mode and under full load on an asphalt road in an open space. The research was conducted in the renewable energy laboratory of Tarbiat-Modares University (TMU). The experiments were carried out at five different intensities of the magnetic field (0 to 4000 gauss) and at five different levels of engine speeds. The measurement of the vibration was a 5 (field intensity) $\times$ 5 (engine speeds) experiment on a randomized design and five replications. The total number of experiments is listed as:

The number of experiments = (5) fuel $\times$ (5) engine speeds $\times$ (5) iterations

Because stationary conditions can be utilized as the basis of measurement to compare vibration in another condition, the experiments in this study included stationary mode. Examination of variance was conducted using the Multi-Factorial Adjusted Show in the SAS 9.3 Measurable Computer program (SAS Institute, Cary, NC, USA). The results of these tests provide recognizable proof of the contrasts in vibrations in response to the fuel and engine speeds. Extra investigations were carried out to independently determine the interaction between the fuel and engine speeds for each treatment. The RMS of speeding up was factually analyzed employing an adjusted two-factorial examination of variance (analysis of variance, ANOVA). In each experiment, the number of five-time domain signals (repeat) with duration of 4 s was recorded with a sampling rate of 120,000.

2.4. The Accelerometers

The acceleration sensor type CTC AC102 was employed to record acceleration signals, and its specifications are presented in Table 2. The output data of the acceleration sensor were converted to digital data using an electronic analog-to-digital converter, and then the digital signals were recorded on a hard drive. The acceleration sensors and vibration measurement setup are illustrated in Figure 2.

Table 2. Specifications of Model AC102 accelerometer manufactured by CTC (USA).

Characteristic	Range
Sensitivity	100 mV/g
Frequency response	0.4 to 14000 Hz
Dynamic range	± 50 g, at peak
Supply voltage	17–31 VDC
Temperature range	-50–120 °C
Natural resonant frequency	26,000 Hz
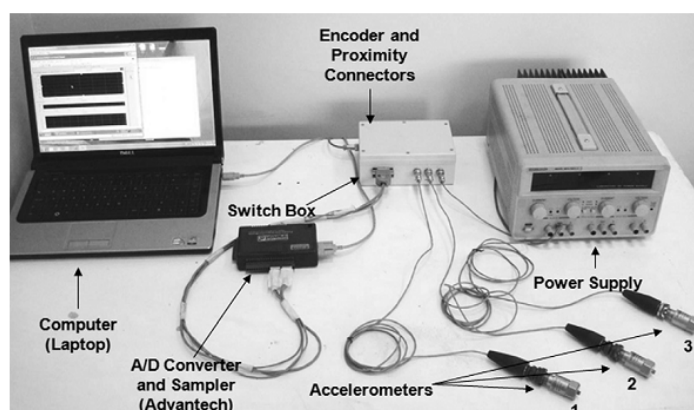
Figure 2. The setup used for the engine vibration measurement.

2.5. Specific Fuel Consumption

Specific fuel consumption is characterized as the mass of the fuel expended to create 1 kWh of genuine engine work. The specific fuel specific fuel consumption may be a comparative variable that shows how an engine changes fuel vitality to real work. In this regard, fuel consumption is accessible in terms of ml/min. Engine-specific fuel consumption was calculated from Equation (1) [18]:

$$\text{SFC} = \frac{60\rho \times \text{FC}}{P} \tag{1}$$

All the tests were repeated three times, and the mean values were reported. The information was measurably analyzed utilizing the two factors completely randomized design in order to study the impacts of engine speeds and fuel types on debilitated outflows and fuel consumption. Furthermore, Duncan's multiple range tests were used to compare the means. It should be noted that the engine was warmed up for about 10 min before measuring the vibration signals for the control sample (0 gauss). For the other experimental runs, the engine was fueled by the magnetized samples for about 10 min before measuring the vibration signals. As a result, for each sample, the engine was stable and the new sample fuel was placed in the fuel circuit.

3. Results and Discussion

3.1. Fuel Specifications

The specifications of pure diesel fuel (0 gauss refers to the condition before magnetic treatment was applied) and diesel fuel magnetized within the permissible range of each item measured in the biodiesel laboratory at TMU are shown in Table 3. As shown, the values obtained for each fuel, including the density, viscosity, and flash point of all fuels, were in the standard range. The 4000-gauss magnetic field intensity provides the lowest value of specific gravity, kinematic viscosity, and flashpoint. With increasing magnetic field intensity, the fuel density reduced, so the lowest density was for the magnetic field of 4000 G. The hypothesis that a magnetic field diminishes the viscosity of many fluids has been reported in the literature [19]. Moreover, a recent report indicated that a magnetic field causes changes in oil viscosity. The results of experiments have shown that the significant reduction in the viscosity of paraffin and crude oil is caused by a combination of long chains [20]. Due to the greater surface area of the combustion chamber, smaller droplets evaporate faster, which causes faster and more complete combustion. In addition, in injection systems (gasoline and diesel), finer fuel droplets increase the combustion speed, and consequently, combustion is more complete [21].

Table 3. Fuel details.

Permissible Range	Accuracy	4000 G	3000 G	2000 G	1000 G	0 G	Fuel Specifications
820–850	± 1 kg/m^3	813.5	815	816	824	826.1	Specific gravity (kg/m^3)
1.9–6	± 0.1 cST	2.43	2.44	2.45	2.51	2.54	Kinematic viscosity at 40 °C (CST)
Max 130	± 1 °C	60.1	62	62.1	64	65.4	Flashpoint (°C)

3.2. Time-Domain Signals

Figure 3 depicts a section of the time domain signal in three directions—lateral, longitudinal, and vertical—at a speed of 1700 rpm and diesel fuel (0 gauss) for the engine under full load. The combustion cycles are shown in this figure. As can be observed, the vibration acceleration in the lateral direction exceeds that in the vertical direction, and the vertical vibration acceleration surpasses that in the longitudinal direction. Therefore, the time domain acceleration signals significantly depend on the direction of measurement. As it is clear the maximum and minimum values of the acceleration signals of vibration recorded at the lateral and longitudinal directions are attributed to the six-cylinder engine being well balanced in the vertical direction than the two other directions. Moreover, the experimental results showed that the time domain acceleration signal values of vibration decrease by applying the magnetic field intensity. Therefore, the value of the time domain acceleration signals using 1000 Gauss field intensity is significantly less than the value of time domain acceleration signals related to fuel without a magnetic field. The reason why acceleration is higher in the lateral direction is the good dynamic balance of the six-cylinder engine, which causes the vibration to reduce on the vertical side than on the lateral one, as well as the blast force produced by the engine in the lateral direction [22].

(**a**)

Figure 3. *Cont.*

(b)
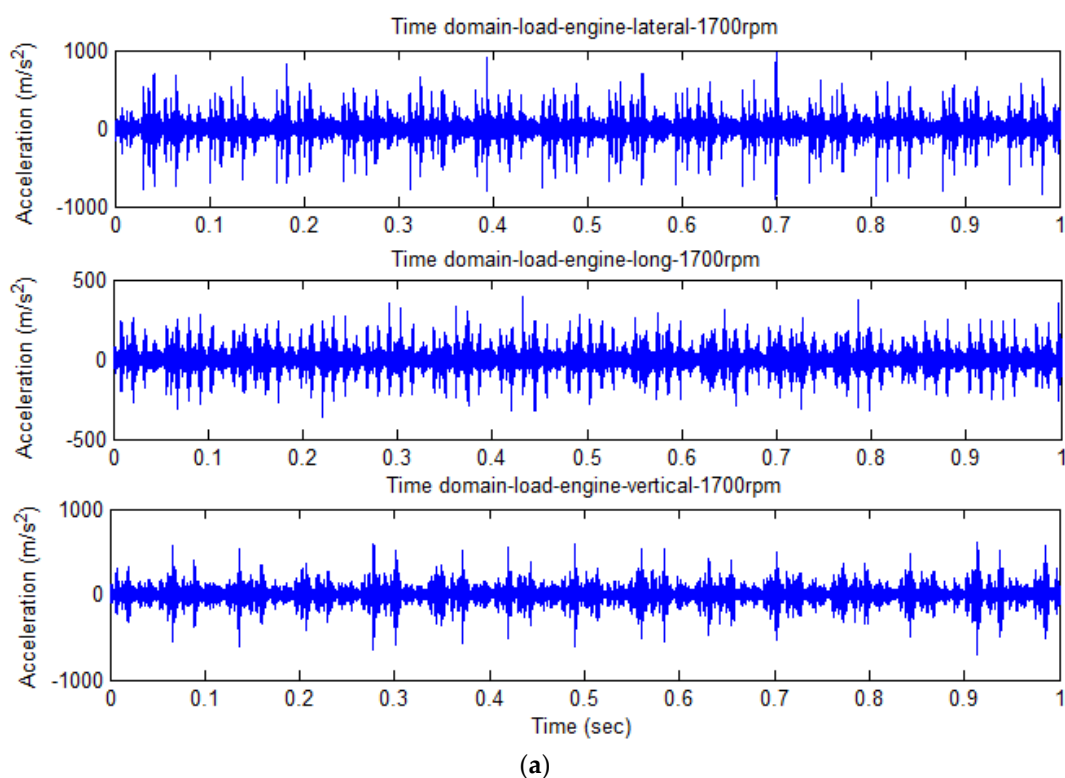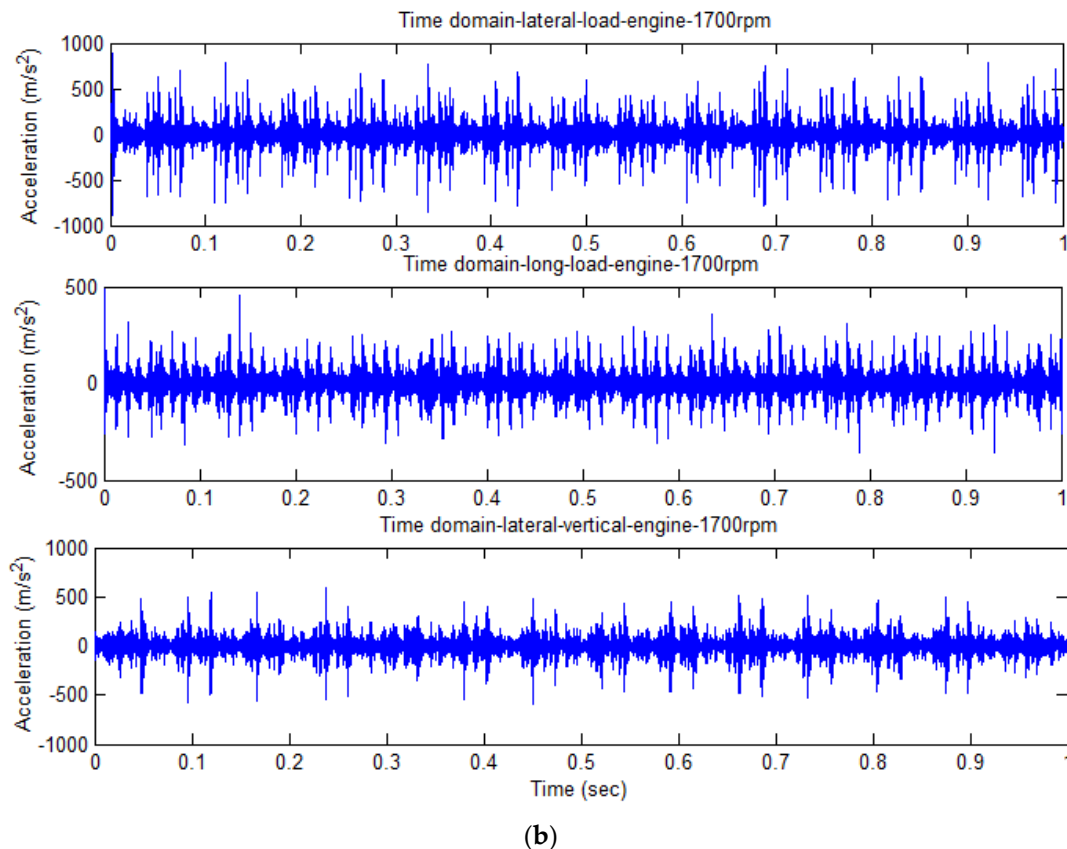
Figure 3. Vibration acceleration signals in the time domain at 1700 rpm engine speed in the lateral, longitudinal, and vertical directions. (**a**) Without a magnetic field. (**b**) Diesel fuel under a 1000-gauss field.

3.3. Evaluation of RMS of Vibration Acceleration Signals

For evaluation of the engine's vibration at different speeds and field intensities applied to fuel, the acceleration RMS was used for each direction of measurement. Five replications against each treatment were considered. Acceleration RMS was calculated using Equation (2):

$$a\mathrm{RMS} = \sqrt{\frac{1}{N}\sum_{k=1}^{N} ak^2} \qquad (2)$$

where a_{RMS} is the root mean square value of the acceleration signal, (m/s^2), a_k is the acceleration amplitude at time of k within the time domain signal, and N, is the entire range of samples (N = 120,000) for 4 s [22].

3.4. Effects of Variable Levels on Vibration

A comparison between the test results for the interaction effects of the direction of measurement and fuel type on RMS is given in Table 4. Duncan's multiple range test was used to compare treatment means. Means were significantly different when $p < 0.01$. For the engine under full load, the RMS significantly affected engine speed (ES) for the longitudinal (x), vertical (z), and lateral (y) axes. The RMS of acceleration increases significantly when the engine speed increases from 1900 to 2100 rpm; this is true for each ES (engine speed) and all axes ($p < 0.05$; Table 3). A similar approach was detailed for the Mitsubishi power tiller [13,16]. As is evident from this table, in the lateral direction, the RMS acceleration values at every level of the fuel are significantly greater than the horizontal and vertical lengths. The reason why acceleration is higher in the lateral direction is the good dynamic balance of the six-cylinder engine, which causes vibration to reduce on the vertical side than on the lateral, and also the existence of blast forces in rotary engines [18]. In the longitudinal

direction, there are no significant differences between RMS values of acceleration for pure diesel fuel at 1000-gauss, and RMS acceleration at 4000 gauss reduced significantly. This could be due to the low intensity of the 1000-gauss field influencing the molecular structure of the fuel. By increasing the field intensity to 4000-gauss, the fuel's molecular structure probably alters, so that the resulting combustion is more uniform. It was clarified that under a fairly powerful magnetic field, hydrocarbon molecules turn into a de-cluster mode with a smaller form, which makes it possible to find more contact space to react with oxygen, and this situation results in a more thorough combustion and fuel consumption decrease [20,23,24]. As regards RMS values of acceleration in the vertical direction, there are significant differences between pure diesel fuel and other fuels, and RMS acceleration reduces significantly at 4000-gauss.

Table 4. RMS acceleration and mean square (MS) comparison derived from a completely randomized design (CRD) and interaction effects of directions and engine speeds.

Applied Field Intensity (FI)	4000 G	3000 G	2000 G	1000 G	0 G
Longitudinal (X)	60.816 [o]	68.816 [n]	71.816 [m]	78.816 [l]	79.816 [l]
Lateral (Y)	97.797 [f]	98.79 [e]	104.729 [c]	119.400 [a]	120.853 [a]
Vertical (Z)	81.040 [r]	84.016 [i]	91.484 [h]	95.167 [g]	96.484 [g,f]

The means with the same letters showed no significant differences ($p > 0.05$).

　　In the longitudinal direction, there is no significant difference between the RMS value of (0 G) fuel acceleration and (1000 G), and with increasing field strength, the acceleration of these fuels slowly decreases. In the vertical direction, too, no significant difference is observed among the RMS values of pure diesel and 1000 G, but compared to other fuels, the RMS value for 2000 G fuel significantly drops and the smallest RMS acceleration value is in the vertical direction. The highest RMS value of acceleration in 1000 G and 0 G fuels is observed in the lateral direction, and the minimum value is in 4000 G fuel in the longitudinal direction. Overall, the RMS of vibration acceleration recorded in the lateral direction is the greatest (average 107.52 m/s^2) and the smallest value is in the longitudinal direction (average 71.23 m/s^2).

3.5. The Interaction Effects of Field Intensity and Engine Speed

　　Table 5 illustrates the evaluation of means for different ES and FS (magnetic field strength). As can be seen, the vibration dramatically rises at 2100 rpm, and the rate of the increase is substantially fast. To discover why vibration increases at some engine speeds, the output torque curve of the engine can be used [25]. The average of increased vibrations for all field intensities from 1700 to 2100 rpm is 2.02, 3.43, 7.65, and 8.57 m/s^2, respectively. Figure 4 illustrates the output torque and power curves performance for Perkins engine model A63544. There are several important points in this diagram. The maximum torque is 431 Nm at 1200 rpm. The maximum power is 82 kW at 2200 rpm. The topmost vibration always occurs at an engine speed where the ES, torque, or power is the greatest. Furthermore, in this engine, the product of power and torque (P-T) reaches the highest engine speed of 2000 rpm. The reason for this claim is this tractor's power take-off [26]. Moreover, Table 5 shows that proportional to the field intensity increase from 0 to 4000 gauss, the average acceleration of vibration reduces by 15%, 15.30%, 12.40%, 12.35%, and 15.38%, respectively (for five ES). This indicates an average 29% reduction in vibration acceleration. The reason why the value of vibration acceleration falls is probably that as the magnetic field increases, the power required to overcome the hydrocarbon clusters of the fuel structure is provided by the engine, as a result of which the fuel burns more constantly and less vibration is produced in the internal parts of the engine [27–31]. Using a magnetic field, the internal energy of fuel can be increased, which means some alteration in the molecular surface of fuel leads to a rise in the internal energy of the fuel, its molecular segregation, and more reactivity, thereby improving combustion [32–34].

Table 5. RMS acceleration and mean square (MS) comparison derived from the completely randomized design (CRD) for each engine speed.

FS	ES (rpm)				
	1700	**1800**	**1900**	**2000**	**2100**
0 G	87.439 [e,f]	91.929 [e]	98.451 [c]	108.598 [b]	118.606 [a]
1000 G	85.111 [f]	87.554 [e,f]	95.505 [d]	107.324 [b]	114.969 [a]
2000 G	81.474 [j,k]	83.561 [j,k]	91.177 [j]	102.875 [g,h]	110.325 [b]
3000 G	79.259 [j]	82.923 [j,i]	90.768 [h]	100.629 [h]	108.795 [g]
4000 G	73.487 [l]	77.867 [k,l]	86.219 [kl]	95.177 [j]	100.356 [h]

The means with the same letters showed no significant differences ($p > 0.05$). Subset for alpha = 0.05.
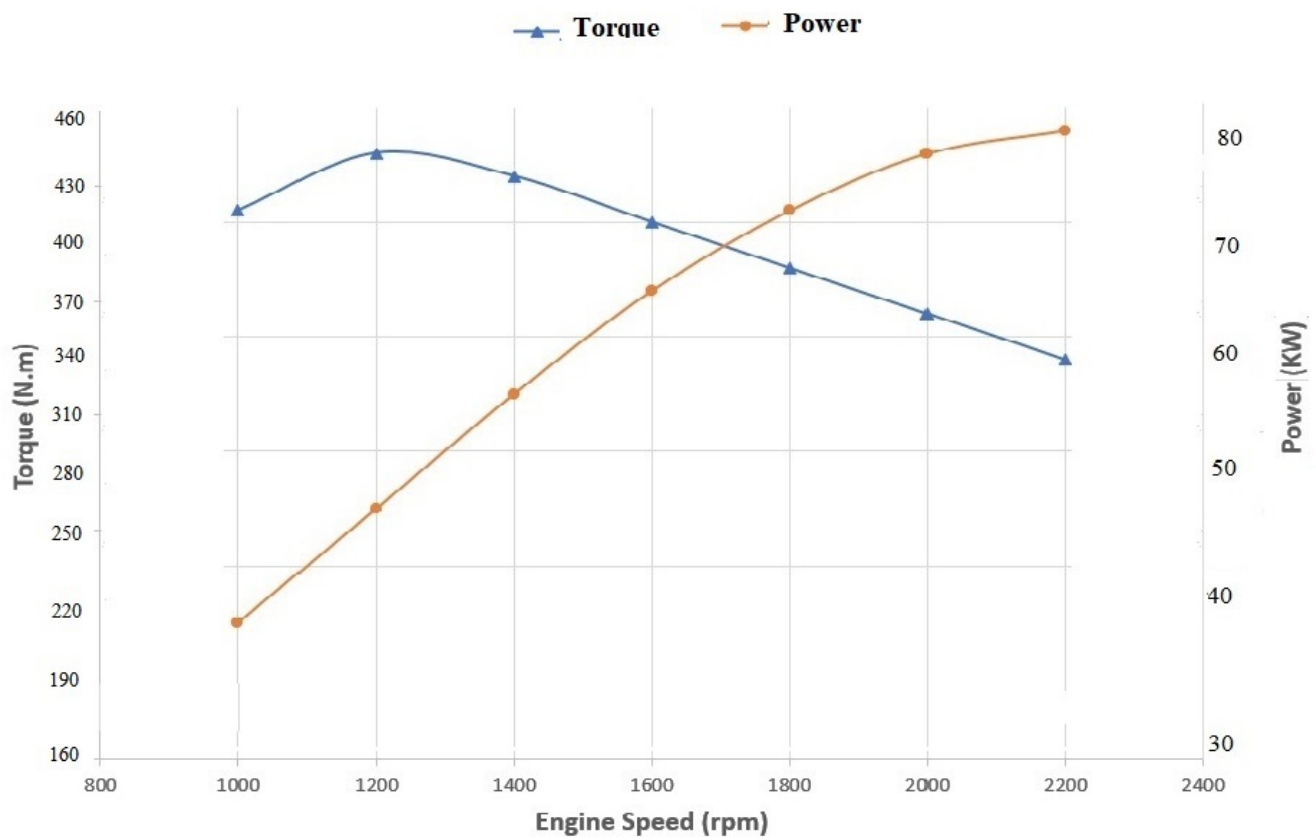
Figure 4. The engine torque power variations in terms of the engine speed.

3.6. Specific Fuel Consumption

Changes in the specific fuel consumption as a function of engine speed are shown in Figure 5. As can be observed in this figure, the diagram of all fuels shows the same trend, while the diagram of 4000 gauss has lower specific fuel consumption.

The maximum amount of specific fuel consumption reduction compared to control fuel was 2.3% for 4000 gauss. The coefficient of determination (R^2) related to the regression equations was fitted and shown on the engine specific fuel consumption data as a function of engine speed for each magnetic field density. Duncan's multiple range tests were used to compare whether the mean values of the engine vibration and specific fuel consumption varied significantly when the engine speed and magnetic field density changed. The results of Duncan's multi-range test are shown in Table 6. Letters (a, b, c, etc.) were utilized to find whether mean values had notable differences at a 0.5% probability level or not using Duncan's multiple range tests. The same letters indicate that there was no remarkable difference at the 0.5% probability level. Moreover, other surveys conducted by scientists

approved the results of this study. For instance, in an investigation, the experimental results showed that the fuel consumption of the diesel engine was less when the engine had a magnetic field than that without it at a higher load. The results showed that consumption of the fuel with a magnetic field was less. The reduction in fuel consumption was about 8% [35].

magnetic fields.	R^2
D100	0.902
1000G	0.918
2000G	0.9427
3000G	0.829
4000G	0.9902
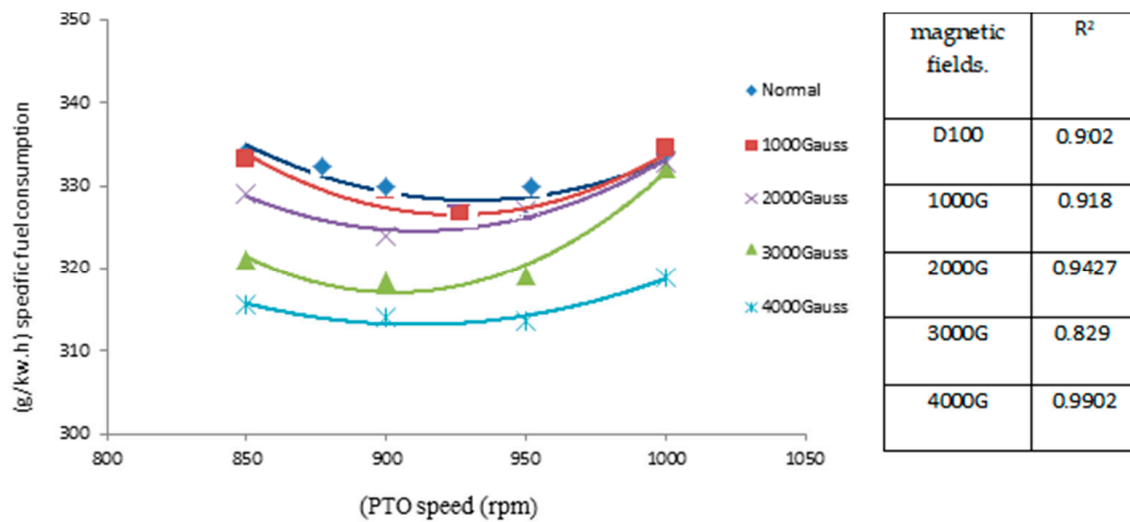
Figure 5. Engine speed and engine specific fuel consumption for different magnetic fields.

Table 6. The magnetic field and SFC.

Magnetic Field (Gauss)	Specific Fuel Consumption (g/kW h)
0 G	330.45 [a]
1000	330.26 [a]
2000	329.296 [a]
3000	326.95 [a,b]
4000	322.6 [b]

The means with the same letters showed no significant differences ($p > 0.05$). Subset for alpha = 0.05.

Table 7 shows Duncan's multi-range test results comparing the average specific fuel consumption and engine speed. As shown, the mean values of specific fuel consumption at speeds of 1700 to 1800 rpm are not significant but significantly decrease at a speed of 1900 rpm. Maximum average specific fuel consumption was seen at a speed of 1700 rpm and 334.86 g/kWh, and minimum average specific fuel consumption was achieved at a speed of 950 rpm and 319 g/kWh.

Table 7. Engine speed and SFC.

Engine Speed (rpm)	Specific Fuel Consumption
1700	334.86 [a]
1800	331 [a]
1900	319 [c]
2000	326 [b]

The means with similar letters showed no significant differences ($p > 0.05$). Subset for alpha = 0.05.

4. Conclusions

In this study, the fuels used included diesel fuel as standard control and fuels that have been subjected to magnetic field intensity at 1000, 2000, 3000, and 4000 gauss. The levels of the magnetic field were selected based on the literature survey as well as the magnetic field ability of the used unit. Some experiments were conducted in this research to evaluate the

effects of magnetic fuel on engine parameters such as engine vibration. Effects of magnetic fields with different intensities were studied on vibration signals of a six-cylinder internal combustion engine. Vibration signals in the longitudinal, vertical, and lateral with 5 levels of engine speed were measured.

From the discussions, it can be concluded that as engine speed increases from 1700 to 2100 rpm, the RMS vibration acceleration average generally increases in all fuels and directions, and this research clarified that by applying a magnetic field to diesel fuel, the MF399 tractor engine vibration significantly decreases provided that the magnetic field density is sufficient.

Moreover, the time domain acceleration signals were significantly dependent on the measurement direction. furthermore, the experimental results showed that the time domain acceleration signal values of vibration decrease by applying the magnetic field intensity. Therefore, the value of the time-domain acceleration signals using a magnetic field intensity was significantly less than the level of acceleration signals related to fuel without a magnetic field.

Along with the engine speed increase from 1700 to 2100 rpm, the RMS average vibration acceleration generally increases in all fuels.

The experimental results showed that the values of RMS vibration acceleration decreases when the magnetic field strength is increased. Therefore, the minimum value of RMS was obtained using a field intensity of 4000 gauss. Moreover, specific fuel consumption declined by about 3/2%.

5. Patents

Patent No. 84531, Title: Magnetic diesel fuel using a magnetizer, Iran Industrial Patent Office.

Author Contributions: Conceptualization, Y.D., S.R.H.-B., and J.M.; methodology, Y.D.; software, Y.D.; validation, S.R.H.-B., H.K., and M.G.; formal analysis, M.G.; investigation, Y.D.; resources, H.K.; data curation, Y.D.; writing—original draft preparation, Y.D.; writing—review and editing, Y.D., M.G. and A.B.; visualization, Y.D.; supervision, S.R.H.-B.; project administration, Y.D.; funding acquisition, S.R.H.-B. All authors have read and agreed to the published version of the manuscript.

Conflicts of Interest: The authors declare no conflict of interest.

Abbreviations

a_{RMS}	Root mean square of acceleration
a_k	Acceleration amplitude at time of k within the time domain signal
FC	Fuel consumption
P	Power
SFC	Special fuel consumption
N	The entire range of samples
ρ	Volumetric mass

References

1. Darvishi, S.; Hassan-Beygi, S.R.; Ghobadian, B.; Massah, J. Magnetizing the perkins A63544 engine fuel and its vibratory assessment. *J. Engine Res.* **2015**, *38*, 17–26.
2. Demirbas, A.H.; Demirbas, I. Importance of rural bioenergy for developing countries. *Energy Convers. Manag.* **2007**, *48*, 2386–2398. [CrossRef]
3. Darvishi, Y.; Hassan-Beygi, S.R.; Zarafshan, P.; Hooshyari, K.; Malaga-Toboła, U.; Gancarz, M. Numerical Modeling and Evaluation of PEM Used for Fuel Cell Vehicles. *Materials* **2021**, *14*, 7907. [CrossRef] [PubMed]

4.　Karami, H.; Rasekh, M.; Darvishi, Y. Effect of temperature and air velocity on drying kinetics and organo essential oil extraction efficiency in a hybrid dryer. *Innov. Food Technol.* **2017**, *5*, 65–75.

5.　Karami, H.; Rasekh, M.; Darvishi, Y.; Khaledi, R. Effect of drying temperature and air velocity on the essential oil content of Mentha aquatica L. *J. Essent. Oil Bear. Plants* **2017**, *20*, 1131–1136. [CrossRef]

6.　Kurji, H.J.; Imran, M.S. Magnetic field effect on compression ignition engine performance. *ARPN J. Eng. Appl. Sci.* **2018**, *13*, 3943–3949.

7.　Sahoo, R.R.; Jain, A. Experimental analysis of nanofuel additives with magnetic fuel conditioning for diesel engine performance and emissions. *Fuel* **2019**, *236*, 365–372. [CrossRef]

8.　Sidheshware, R.K.; Ganesan, S.; Bhojwani, V.K. Enhancement of internal combustion engine efficiency by magnetizing fuel in flow line for better charge combustion. *Heat Transf. Res.* **2020**, *51*, 419–431. [CrossRef]

9.　Faris, A.S.; Al-Naseri, S.K.; Jamal, N.; Isse, R.; Abed, M.; Fouad, Z.; Kazim, A.; Reheem, N.; Chaloob, A.; Mohammad, H. Effects of magnetic field on fuel consumption and exhaust emissions in two-stroke engine. *Energy Procedia* **2012**, *18*, 327–338. [CrossRef]

10.　Thiyagarajan, S.; Sonthalia, A.; Edwin Geo, V.; Ashok, B.; Nanthagopal, K.; Karthickeyan, V.; Dhinesh, B. Effect of electromagnet-based fuel-reforming system on high-viscous and low-viscous biofuel fueled in heavy-duty CI engine. *J. Therm. Anal. Calorim.* **2019**, *138*, 633–644. [CrossRef]

11.　Govindasamy, P.; Dhandapani, S. Effects of EGR & magnetic fuel treatment system on engine emission characteristics in a bio fuel engine. In Proceedings of the International Conference on Mechanical Engineering, Dhaka, Bangladesh, 26–28 December 2009; pp. 26–28.

12.　Tao, R.; Xu, X. Viscosity reduction in liquid suspensions by electric or magnetic fields. *Int. J. Mod. Phys. B* **2005**, *19*, 1283–1289. [CrossRef]

13.　Marsili, A.; Ragni, L.; Santoro, G.; Servadio, P.; Vassalini, G. PM—Power and machinery: Innovative systems to reduce vibrations on agricultural tractors: Comparative analysis of acceleration transmitted through the driving seat. *Biosyst. Eng.* **2002**, *81*, 35–47. [CrossRef]

14.　Khan, N.S.; Shah, Q.; Sohail, A.; Kumam, P.; Thounthong, P.; Muhammad, T. Mechanical aspects of Maxwell nanofluid in dynamic system with irreversible analysis. *ZAMM-J. Appl. Math. Mech. Z. Angew. Math. Mech.* **2021**, *101*, e202000212. [CrossRef]

15.　Khan, N.S.; Humphries, U.W.; Kumam, W.; Kumam, P.; Muhammad, T. Assessment of irreversibility optimization in Casson nanofluid flow with leading edge accretion or ablation. *ZAMM J. Appl. Math. Mech. Z. Angew. Math. Mech.* **2022**, *102*, e202000207. [CrossRef]

16.　Ahmadian, H.; Hassan-Beygi, S.R.; Ghobadian, B. Power tiller vibration acceleration envelope curves on transportation mode. *J. Vibroeng.* **2013**, *15*, 1431–1441.

17.　Rocha, N.; González, C.; Marques, L.C.d.C.; Vaitsman, D.S. A preliminary study on the magnetic treatment of fluids. *Pet. Sci. Technol.* **2000**, *18*, 33–50. [CrossRef]

18.　Taghizadeh-Alisaraei, A.; Ghobadian, B.; Tavakoli-Hashjin, T.; Mohtasebi, S.S. Vibration analysis of a diesel engine using biodiesel and petrodiesel fuel blends. *Fuel* **2012**, *102*, 414–422. [CrossRef]

19.　Okoronkwo, C.; Nwachukwu, C.; Ngozi–Olehi, L.; Igbokwe, J. The effect of electromagnetic flux density on the ionization and the combustion of fuel (an economy design project). *Am. J. Sci. Ind. Res.* **2010**, *1*, 527–531. [CrossRef]

20.　Saksono, N. Magnetizing kerosene for increasing combustion efficiency. *J. Teknol. Ed.* **2005**, *2*, 155–162.

21.　Dhandapani, S. Theoretical and Experimental Investigation of Catalytically Activated Lean Burnt Combustion. Ph.D. Thesis, Indian Institute of Technology, Chennai, India, 1991.

22.　Taghizadeh, A.A.; Tavakoli, H.T.; Ghobadian, B. An Analysis and Evaluation of Vibrations of Power Tiller in the Stationary Conditions. *Iran. J. Biosyst. Eng.* **2010**, *41*, 279677.

23.　Faraji, H.; Heidarbeigi, K.; Samadi, S. Effect of magnetized ethanol-gasoline blends on vibration and sound emissions of a single cylinder SI engine. *Res. Sq.* 2020. [CrossRef]

24.　Kita, R.J.; Kulish, P.A. Electromagnetic Device for the Magnetic Treatment of Fuel. U.S. Patents US5829420A, 3 November 1998.

25.　Langer, T.H.; Ebbesen, M.K.; Kordestani, A. Experimental analysis of occupational whole-body vibration exposure of agricultural tractor with large square baler. *Int. J. Ind. Ergon.* **2015**, *47*, 79–83. [CrossRef]

26.　Zhang, J.; Yao, H.; Chen, L.; Zheng, E.; Zhu, Y.; Xue, J. Vibration characteristics analysis and suspension parameter optimization of tractor/implement system with front axle suspension under ploughing operation condition. *J. Terramech.* **2022**, *102*, 49–64. [CrossRef]

27.　Pera, I. Magnetizing Hydrocarbon Fuels and Other Fluids. U.S. Patent 4716024A, 29 December 1987.

28.　Munpollasri, S.; Poo-arporn, Y.; Donphai, W.; Sirijaraensre, J.; Sangthong, W.; Kiatphuengporn, S.; Jantaratana, P.; Witoon, T.; Chareonpanich, M. How magnetic field affects catalytic CO_2 hydrogenation over Fe-Cu/MCM-41: In situ active metal phase—Reactivity observation during activation and reaction. *Chem. Eng. J.* **2022**, *441*, 135952. [CrossRef]

29.　Jiancun, G.; Xigang, Y.; Shoutao, H.; Le, W.; Zijin, H.; Xu, S.; Ruxia, L. Effects of Magnetic Fields on Combustion and Explosion. *Chem. Technol. Fuels Oils* **2022**, *58*, 379–390. [CrossRef]

30.　Liu, X.; Xie, N.; Xue, J.; Li, M.; Zheng, C.; Zhang, J.; Qin, Y.; Yin, Y.; Dekel, D.R.; Guiver, M.D. Magnetic-field-oriented mixed-valence-stabilized ferrocenium anion-exchange membranes for fuel cells. *Nat. Energy* **2022**, *7*, 329–339. [CrossRef]

31. Niaki, S.R.A.; Zadeh, F.G.; Niaki, S.B.A.; Mouallem, J.; Mahdavi, S. Experimental investigation of effects of magnetic field on performance, combustion, and emission characteristics of a spark ignition engine. *Environ. Prog. Sustain. Energy* **2020**, *39*, e13317. [CrossRef]
32. Attar, A.; Arulprakasajothi, M.; Vasulkar, D.; Gorde, N.; Kharat, S.; Kulkarni, S. Investigation of impact of the magnetic field through halbach array on Hydrocarbon fuel. *Int. J. Ambient. Energy* **2022**, *43*, 2124–2129. [CrossRef]
33. Sidheshware, R.K.; Ganesan, S.; Bhojwani, V. Experimental investigation on the viscosity and specific volume of gasoline fuel under the magnetisation process. *Int. J. Ambient. Energy* **2022**, *43*, 486–491. [CrossRef]
34. Zhou, S.; Gao, J.; Luo, Z.; Hu, S.; Wang, L.; Wang, T. Role of ferromagnetic metal velvet and DC magnetic field on the explosion of a C3H8/air mixture-effect on reaction mechanism. *Energy* **2022**, *239*, 122218. [CrossRef]
35. Patel, P.M.; Rathod, G.P.; Patel, T.M. Effect of magnetic field on performance and emission of single cylinder four stroke diesel engine. *IOSR J. Eng.* **2014**, *4*, 28–34. [CrossRef]